ARTICLES

Combined Small-Angle X-ray and Neutron Scattering Experiments for Thickness Characterization of Ganglioside Bilayers

L. Cantù,[†] M. Corti,*[,†] E. Del Favero,[†] M. Dubois,[‡] and Th. N. Zemb[‡]

Dipartimento di Chimica e Biochimica Medica - INFM, Università di Milano, LITA, via F.lli Cervi 93, 20090 Segrate, Italy, and Service de Chimie Moléculaire, CEA Saclay, Bat 125, 91191 Gif sur Yvette, France

Received: July 17, 1997; In Final Form: April 22, 1998

Combined small-angle neutron and X-ray scattering experiments on dilute solutions of the ganglioside GM3 in water are presented. The contrast profiles along the lipid and sugar portions of the ganglioside molecule for the two types of radiations are different, a feature which, added to the extension of the scattering q range to $q \sim 0.4$ Å^{-1}, allows an accurate determination of the cross section of the bilayer in dilute solution. The electronic density profile of the bilayer cross section can be interpreted only by assuming thickness fluctuations, which have already been theoretically predicted for the GM3 bilayers, due to the peculiar packing properties of the monomer. Increasing temperature from room temperature to 50 °C has the effect of flattening the GM3 bilayer, as the thickness and the water content of the outer hydrophilic layer decrease, while the thickness of the inner hydrophobic region is almost unchanged.

Introduction

Gangliosides are an interesting class of natural glycosphingolipids occurring in plasma membranes.[1] They have a double-tailed lipid portion, like phospholipids, constituted by a sphingosine and a fatty acid with an average of 20 carbons each and a bulky headgroup made up of several sugar rings and sialic acids.

As biological amphiphiles, gangliosides associate in aqueous solution, with the interesting feature of giving rise to different aggregated structures according to the length and ramification of their hydrophilic portion.[2]

In principle, the extended double-tailed hydrophobic part assigns gangliosides to the family of membrane-forming amphiphiles. Indeed, the gangliosides GM4 and GM3,[3] with two and three sugar rings in the headgroup, form spontaneous vesicles in binary dilute solutions.[4,5] Nevertheless, for gangliosides of higher complexity than GM3, the role played by the hydrophilic part of the molecule becomes very important. For instance, for GM2, which has four sugar rings, and for gangliosides with a larger number of sugars, the hydrophilic headgroup is so extended that micelles are formed instead of vesicles, despite the presence of a double hydrophobic tail.[5−7]

The ganglioside GM3 is interesting because it is at the border of the vesicle-to-micelle transition in the ganglioside series. It has the peculiar feature to form vesicles spontaneously, in thermodynamic equilibrium, in water at normal pH, independently of added salts, and without supply of external energy.[8] Moreover, unlike the classically studied phospholipids, vesicles formed by pure GM3 have been found, on the basis of light scattering results, to be involved in dynamic rearrangement. Closed vesicles form and break rapidly in thermodynamic equilibrium with a small amount of lamellar fragments of finite size.[8,9] On one hand, spontaneous vesiculation is somehow unexpected, since a single amphiphile bilayer, like the one formed by GM3 in water, is forcedly symmetric in composition, so that its spontaneous curvature is zero. Therefore, flat lamellar structures should be energetically favored, in this respect, as some energy cost should be paid to bend such a bilayer into a closed vesicle. On the other hand, due to the lipid exposure to water occurring at the edges, the lamellar fragments are energetically unfavored. The coexistence of open bilayers and closed vesicles arises therefore from the fact that the free energy of the two types of aggregate are equivalent, by compensation of border effects and bending effects.

Indeed, vesicles are strongly favored when a second ganglioside is added, as has been observed by mixing GM3 with GM1, a ganglioside with a larger headgroup.[10] In the case of mixed gangliosides with different headgroup volumes, spontaneous curvature readjustments of the two back-to-back monolayers via demixing can give rise to a finite spontaneous curvature of the bilayer, favoring energetically, vesicles over other structures.

Until now, only the peculiar ensamble properties of GM3 solutions have been studied and described. Some features of the bilayer at the molecular level have also been theoretically predicted, like the existence of persistent squeezing deformations reasonably connected to the mismatch in the lateral hindrances of the hydrophobic and hydrophilic parts of the GM3 monomer.[11] Some experimental information about local properties of the GM3 bilayer, like its total and partial thicknesses, is needed in order to complete the description of the system as well as to have a better understanding of the molecular packing properties which give rise to the observed behaviors.

The aim of this paper is to determine GM3 bilayer thick-

* Corresponding author: E-mail mario.corti@unimi.it.
[†] Università di Milano.
[‡] CEA Saclay.

S1089-5647(97)02341-9 CCC: $15.00
Published on Web 07/03/1998

nesses, and their behavior versus temperature, by means of a high-resolution scattering study, using SAXS and SANS as independent experiments on the same samples. The combined use of the two techniques is convenient, since the contrast profile along the lipid and sugar portions of the ganglioside molecule for the two types of radiations is different. The contemporary analysis of the results, which have to match on the same model, allows to get a more detailed description of the system.[12] It has been shown on the example of SDS[13] that extending the q range of measurements beyond 0.4 Å^{-1} allows the determination of the partial thicknesses of the polar and apolar layers. Of course, since the bare experimental resolution is about $2\pi/q_{max}$, that is only $\cong$10 Å even in the extended q range case, the precise determination of the partial thicknesses needs the scattering results to be integrated by some reasonable information about the system. Since the pioneering work of Hayter and Penfold,[14] it is known that the most efficient constraint concerns molecular volumes: layer thicknesses and scattering length densities are by no means independent variables, since they are linked by the fact that bilayers are made of molecules of known partial molar volumes.[15−17]

In the case of usual flat bilayers, as well as for usual micelles, the use of molecular constraints on a well-assessed model for packing allows both an accurate determination of their partial thicknesses and a good estimate of the water content of the hydrophilic layer. It should be stressed that this sort of "hydration", which can be inferred by scattering experiments, is a purely steric variable: it is the number of water molecules per amphiphile molecule that has to be included in the polar layer in order to account for its scattering length density and thickness. This volumetric determination is by no means sensitive to the binding energy of the water molecules to the hydrophilic headgroups which, if needed, has to be determined by a thermodynamic method, as in osmotic pressure experiments.[18]

The measurements presented in this paper were performed as a function of temperature, which is known to induce interesting and unexpected effects on ganglioside molecules and aggregates, including conformational changes in the oligosaccharide headgroups, as has been observed for micelle-forming gangliosides.[19,20]

Materials and Methods

Sample Preparation. The ganglioside GM3, prepared as sodium salt, was extracted, purified, and chemically characterized as described in ref 21. The dry powder was dissolved in a 30 mM NaCl−D_2O solution at a concentration of 3 mM. The molecular weight of GM3 is 1195.. NaCl was added to shield Coulomb interactions among aggregates.[22] The same GM3 samples were used for both neutron and X-ray scattering experiments.

Small-Angle X-ray Scattering (SAXS) Experiments. Experiments of small-angle X-ray scattering on GM3 solutions were performed in pinhole geometry, using a Huxley-Holmes camera described in ref 23. The Cu Kα line was used as incident radiation, with a 12 kW rotating anode. Samples were kept in measuring capillaries, made of Lindemann glass, with an inner diameter of 1.5 mm. Typical counting times were 12 h per sample, using a 2D gas detector, calibrated as described by Né et al.[24] This procedure allows to obtain reproducibility in routine measurements of scattering intensities, in the range of 0.01 cm^{-1}. Water was used as reference, giving a constant scattering intensity of 0.016 cm^{-1}, as expected from its electronic density and compressibility at room temperature. Resolution effects imposed by pinhole scattering geometry are irrelevant, as reported in ref 23.

TABLE 1: Volume and Contrast Data for the GM3 Molecule[a]

moiety	mol vol (Å^3)	electron density (electrons/Å^3)	neutron sld (10^{10} cm^{-2})
GM3 headgroup	646	0.538	3.6
GM3 tail	1066	0.297	−0.4
D_2O	30	0.33	6.35

[a] The molecular volumes, electron density, and neutron scattering length density are reported for the GM3 hydrophilic and hydrophobic moieties. Data for D_2O are also recalled.

Small-Angle Neutron Scattering (SANS) Experiments. Experiments of small-angle neutron scattering were performed on PAXE setup at L.L.B. Orphée using two different wavelengths, 5 and 10 Å, and a range of momentum transfer $q = (4\pi/\lambda)\sin(\theta/2)$ between $q_{min} = 0.003$ Å^{-1} and $q_{max} = 0.2$ Å^{-1}, with θ the scattering angle. The resolution of the wavelength selector was $\Delta\lambda/\lambda = 10\%$. The resolution correction which has to be accounted for in the data treatment due to 10% wavelength distribution is relevant only if the scattering pattern contains peaks or oscillations. Otherwise, if the scattering spectrum shows a monotonic behavior, the correction due to $\Delta\lambda/\lambda = 10\%$ is irrelevant. Absolute scaling was made according to the method introduced by Cotton,[25] by using a separate measurement of the absolute number of neutrons passing through the sample during the experiment.

To be compared to model predictions, both SAXS and SANS data were rescaled by the invariant Q^*.[26] Q^*, defined as

$$Q^* = \int_0^\infty I(q)q^2\,\mathrm{d}q \tag{1}$$

was calculated by using the experimental $I(q)$ in the available q range, while the upper part, extending beyond q_{max}, was evaluated using a Porod extrapolation for $I(q)$. The lower part of the integral is approximated by a triangle, the area of which is $(I(q_{min})q_{min}^3)/2$. On the other hand, in the case of the three-contrast system constituted by the amphiphilic bilayer in water, the value of the invariant is given by

$$Q^* = 2\pi[\Phi_1(\Phi_2\Delta\rho_{21}^2 + \Delta\rho_{31}^2) + \Phi_2(\Phi_1\Delta\rho_{21}^2 + \Delta\rho_{32}^2) + \Phi_2\Delta\rho_{31}^2 + \Phi_1\Delta\rho_{32}^2] \tag{2}$$

where Φ_1 and Φ_2 are the volume fractions of the hydrocarbon and sugar moieties and $\Delta\rho_{ij}$ represents the contrast differences between media i and j, with 1 and 2 indicating the lipid and the hydrated sugar parts, respectively, and with 3 the surrounding water. Equation 2 is valid whatever the microstructure of the solution, with the only underlying assumption that aggregates are made of two media separated by sharp edges from each other and from the surrounding water. The expected value of Q^* can be calculated from known quantities. In fact, the volume fractions Φ_1 and Φ_2 are obtained from the known GM3 concentration and from the partial specific volumes of the two parts of the amphiphilic molecule, while the contrast differences are known from the chemical composition and, again, from the partial specific volumes. The contrast terms, different for SAXS and SANS, are given by the electron densities in the case of X-rays and by the scattering length densities in the case of neutrons. Table 1 summarizes the volume and contrast data for the GM3 molecule.

The scattered intensity for a statistically isotropic dispersion of large flat aggregates of constant thickness is given by[27]

$$I(q) = \frac{4\pi}{q^2}\Sigma\left[t_1\Delta\rho_{12}\frac{\sin(qt_1)}{qt_1} + t_2\Delta\rho_{23}\frac{\sin(qt_2)}{qt_2}\right]^2 \qquad (3)$$

where $2t_1$ and $2t_2$ are the hydrophobic and the total thicknesses of the bilayer, respectively, and Σ is the specific area of the bilayer.

For a flat bilayer, according to the molecular modeling, giving the area per molecule σ measured at the hydrophobic−hydrophilic layers interface imposes the half-thicknesses of the bilayer t_1 and t_2 to be

$$t_1 = V_L/\sigma \quad \text{and} \quad t_2 = t_1 + (V_S + hV_W)/\sigma \qquad (4)$$

where the sum of the hydrophobic and hydrophilic molecular volumes, V_L and V_S, is equal to the volume of the GM3 monomer, as measured by densitometry (1712 Å^3 per molecule), and V_W is 30 Å^3. In eq 3, the specific area Σ is imposed by the amphiphile concentration c_s (number of GM3 molecules per Å^3) as $\Sigma = c_s\sigma$. The fit can then be tried with the two fitting parameters area per headgroup σ and "hydration" h, for both the SANS and SAXS results, provided that the proper contrast terms are used for the two types of radiation.

Results and Discussion

(a) Bilayer Geometrical Parameters. The X-ray and neutron scattering intensity measurements as a function of the modulus of the scattering vector q, performed on the same 3 mM GM3 solution at a temperature of 20 °C, are reported in Figure 1, a and b, respectively. The two scattering curves are qualitatively different: the pronounced oscillations of the X-ray spectrum are absent in the neutron spectrum. This is due to the internal inhomogeneity of the aggregates which gives rise to a nonconstant contrast profile which is different for the two types of radiation.

The information about the system can be extracted from the experimental data either by molecular model fitting or by the well-known indirect Fourier transform (IFT) method.[28]

After the assumption of a shape, the molecular model fitting requires only few parameters, that is, in the case of flat bilayers, the area per molecule (σ) and the number of water molecules (h) per amphiphile molecule. Then, with these two parameters, full X-ray and neutron spectra have to be reproduced correctly, taking into account the molecular volume constraints.

Procedures including the Fourier transform method require scattering functions measured in a large q range to avoid truncation effects and require the final results to be carefully tested for molecular consistency since, as no molecular constraint is imposed on the scattering object, unphysical solutions can be obtained and have to be discarded.[29] Anyway, the complete algorithm of unrestricted inversion of data toward real space in the general case has been recently described in ref 30.

For this study, focused on the determination of the transverse cross section of the bilayer, we decided to use both methods to determine the GM3 bilayer partial and total thicknesses and to compare the final results, which should be similar provided that systematic errors due to edge effects are minimized. In fact, deviations from the infinite-lamella behavior show up at low q values, where the finite dimension of the aggregates (vesicles with radius ∼250 Å) plays a role, while information about the bilayer cross section can be gained by looking at the high q range of the scattering spectra. Therefore, the experimental data, such as those shown in Figure 1a,b, obtained in the range $q >$ 0.03 Å^{-1}, were both fitted using molecular constraints and Fourier inverted.

The best molecular model fit to the SANS data by means of eq 3 is obtained with an area per molecule $\sigma = 70$ Å^2. All experimental data lie in a region bound by the two curves corresponding to ±10% variations in σ. This value for σ in the GM3 vesicle bilayer is compatible with typical values in the monolayer as found at the air−water interface in the expanded liquid region.[31] If treated as usual flat bilayers of constant thickness and clear-cut separation between polar and apolar layers, the molecular constraints expressed in eq 4 evaluates the GM3 bilayer total apolar thickness to be $2t_1 = 30$ Å.

Of the two parameters, σ and h, required in the molecular model fitting, the only one that affects sensibly the simulation of the SANS results is the surface area per molecule σ at the lipid−sugar interface of GM3, due to the features of the contrast profile in the case of neutron scattering. On the other hand, the number h of water molecules associated with each oligosaccharide chain in the external parts of the bilayer can be tuned in order to reproduce the high-q oscillations observed in the SAXS measurements. The overall shape of the experimental SAXS spectrum is reproduced with the correct position of minima and maxima by using the value $\sigma = 70$ Å^2 determined from SANS measurements fitting and assigning $h = 24 \pm 3$. Thickness polydispersity or fluctuations in the real bilayers prevent the experimental SAXS data from showing the strictly zero minima which are theoretically predicted for model bilayers.

In the same q range, the same SAXS and SANS experimental data were analyzed according to the indirect Fourier transform method[28] and subsequently deconvoluted as indicated in ref 30 to get the scattering density profile. Sixteen splines and a maximum distance in real space of 100 Å for the cross section were used. It has to be noted that restricting the q range to $q >$ 0.03 Å^{-1}, which is to a length scale where the GM3 bilayer can be forgotten to be curved up in vesicles, induces the absence of oscillations in the Patterson function, consistent with the molecular fitting results. Eight levels of contrast were allowed in the inversion process. The full lines in Figure 1a,b represent reconstructed SAXS and SANS intensities due to lamellar sheets with the contrast profiles reported as full lines in Figure 2a,b as obtained trough the procedure involving the IFT method. The dotted lines in Figure 2a,b draw the contrast profiles obtained by allowing only two levels of contrast in the inversion procedure, while the thick lines show the ones beared by the results of the molecular model fitting procedure. The final results in terms of cross section (and consequently the reconstructed intensities), as obtained with the two well-established methods for data evaluation, are equivalent. This is of course expected, as they represent the same system and, moreover, are extracted from the same experimental data, and then constitutes a test that no spurious effects have been introduced by the choice of restricting the q range for fitting.

Let's now turn to the numerical values, that is, to discuss the cross section description reported in Figure 2a,b, on which the two distinct methods for data treatment reasonably agree. Let us recall that, according to the currently accepted models, an usual bilayer, made up by two back-to-back layers, has total and apolar half-thicknesses, t_2 and t_1, corresponding to the length of the whole amphiphilic molecule and of its hydrophobic tail, respectively, while the two external polar sheets have a thickness $t_2 - t_1$ equivalent to the length of the hydrophilic headgroup. A comparison between the set of parameters deduced from the experimental data ($t_2 = 36$ Å, $t_1 = 15$ Å) and the dimension of

the GM3 molecule reveals that this current model is too simple to describe the GM3 bilayer.

In fact, the half-thickness of the GM3 bilayer is found to be $t_2 = 36$ Å, a distance from the midplane which can be covered by the GM3 monomer, if fully extended, that is, paying the 24 Å extended length of the hydrophobic chains plus the 12 Å extended length of the sugar headgroups. What needs to be carefully considered is how can the three sugars of the GM3 headgroup extend over a distance of ≈20 Å from a lipid surface at $t_1 \cong 15$ Å to the external surface at t_2. The fact that t_1 is much lower than the length of the hydrophobic tail is not unrealistic by itself, as it can be accounted for by considering interdigitation or chain folding, but the total thickness should be reduced accordingly. The only possible explanation for this strange contrast profile is to assume that the GM3 bilayer is not at all an usual flat bilayer.

A picture can be imagined in which the GM3 bilayer is affected by strong thickness fluctuations in the form of peristaltic deformations, in such a way that the average cross section profile is made by an inner step roughly accounting for an average lipid thickness plus a wide outer step accounting for thickness fluctuations. The inner step half-thickness is much lower than the 24 Å extended length for the GM3 monomer apolar chains which constitute the contribution needed to cover the assessed t_2 and also lower than their 19 Å flexible length, while the outer step half-thickness is much wider than the ≈12 Å extended length of a three-sugar linear chain. As far as the contrast is concerned, both water and lipid would contribute to modify the value of the contrast in this outer volume with respect to the one of sugar headgroups. For example, in the case of SAXS measurements, which are much more sensitive to this outer layer, the presence of either water or lipid would play a role in decreasing the contrast. Moreover, the presence of thickness fluctuations could explain why such a large amount of water (≈24 molecules per monomer with only three sugars) is to be put in the outer layer, modeled as a flat one, to reconstruct its contrast while filling a big volume.

Such thickness fluctuations, also in the form of permanent deformations, have been theoretically predicted for the GM3 bilayer, as a consequence of the energy difference between concave and convex deformations of each of the two monolayers, originating from the mismatch in the lateral hindrance of the GM3 monomer headgroup and chains.[11,32]

Another possibility that can be considered to give rise to a thickness of the outer layer extending beyond headgroup dimension, as experimentally determined, is individual molecular protrusion, rather than collective peristaltic motion.

From an energetic point of view, following the evaluations of Podgornik and Parsegian,[33] neither collective peristaltic motion nor single-molecule protrusion can be excluded a priori. From the experimental point of view, unfortunately, the high-q part of the scattering spectra cannot distinguish between these two mechanisms. Nevertheless, one of these mechanisms has to be the origin of the large average outer thickness of the GM3 bilayer.

As far as the general characterization of the GM3 bilayer is concerned, the bilayer could be deformed also by undulations at constant thickness, but they cannot be assessed with the kind of experiment that has been performed in this study. One of the direct experimental methods used to reveal bilayer undulations has been developed for lamellar phases and consists of measuring the power-law decay of the Bragg peaks appearing in their X-ray spectra.[15] Anyway, for GM3, as happens for bilayers of other charged surfactants,[23] the Bragg peak broadening is not measurable using conventional SAXS experiments.

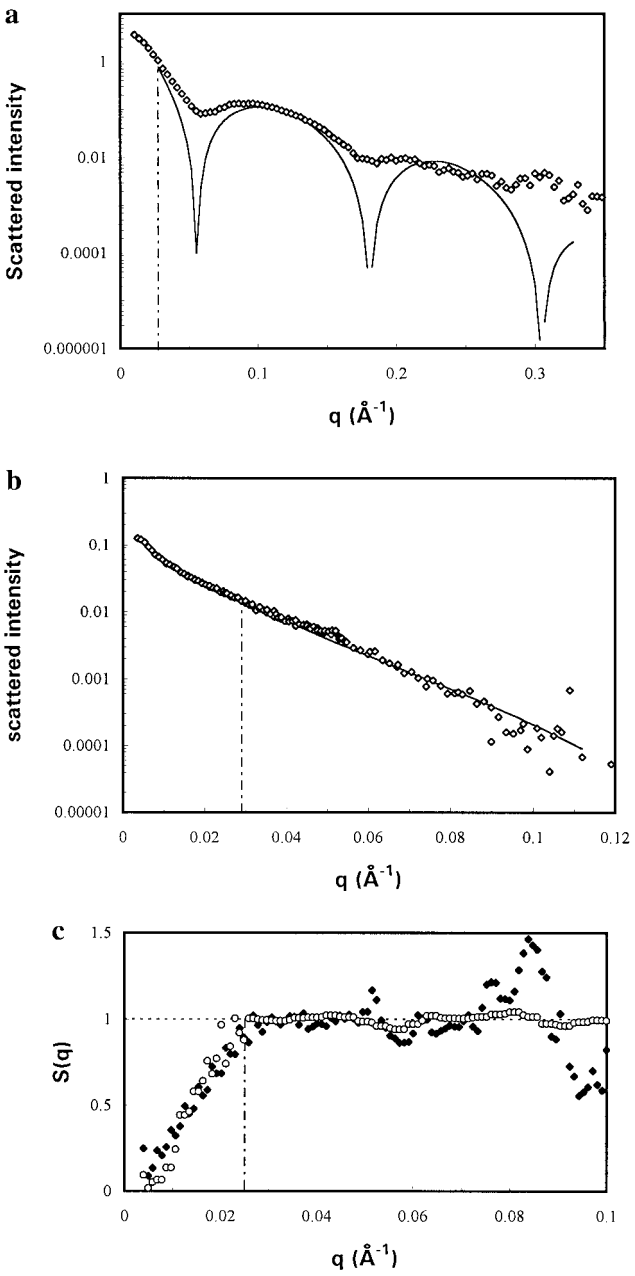

Figure 1. SAXS (a) and SANS (b) spectra obtained for the 3 mM GM3 solution at low temperature. The thick line represents the reconstructed intensities due to lamellar sheets with the contrast profiles reported as full lines in Figure 2. The dashed−dotted vertical line roughly identifies the lower limit of the q range used for thickness determination, as described in the text. (c) The systematic difference at low q between the experimental results and the simulated data for infinitely extended planar sheets, here evidenced by their ratio $S(q)$ both for SANS (full diamonds) and SAXS (open circles), is expected as a consequence of the existence of an in-plane coherence length ξ, that is, at large scales as compared to the bilayer cross section ($\gg 2t_2$), the GM3 bilayers are curved up in vesicles, and, in general, bilayers are randomly folded. The cutoff at $q_0 = 0.025$ Å^{-1} indicates that, for GM3, $\xi = 2\pi/q_0$ is of the order of 250 Å, indeed, as the radius of the GM3 vesicles.

It is interesting to recall here two experimental observations made on an amphiphile of the same class of GM3, the five-sugar headgroup GM1, either arranged in monolayers as studied in a surface-force machine by Parker[34] and later by Wood et al.[35] as well as inserted in a lamellar phase of phosphatidyl-

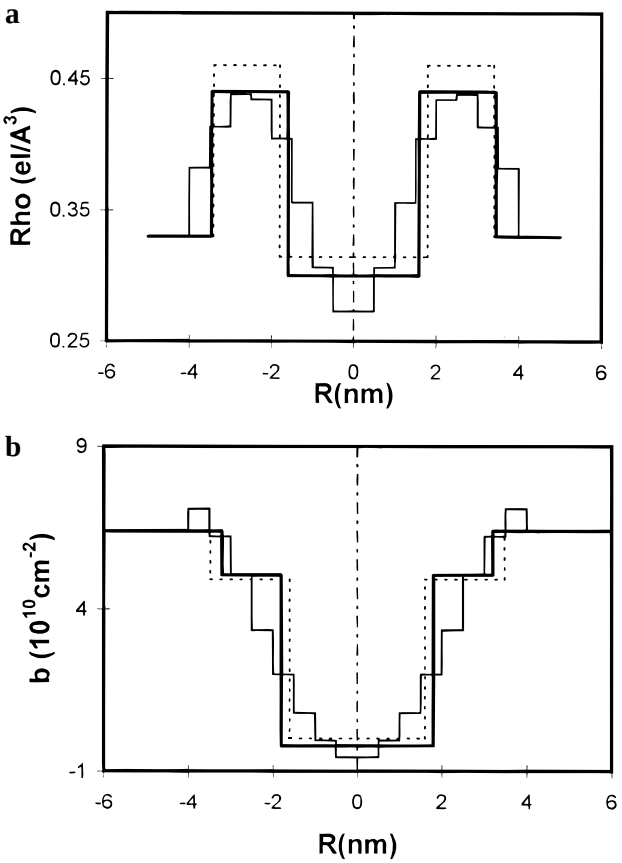

Figure 2. Contrast profiles obtained for the GM3 bilayer at low temperature in the case of SAXS (a) and SANS (b). The results of three analysis modes are reported together: thick lines, two-level model fitting; thin lines, eight-level IFT method; dotted lines, two-level IFT method.

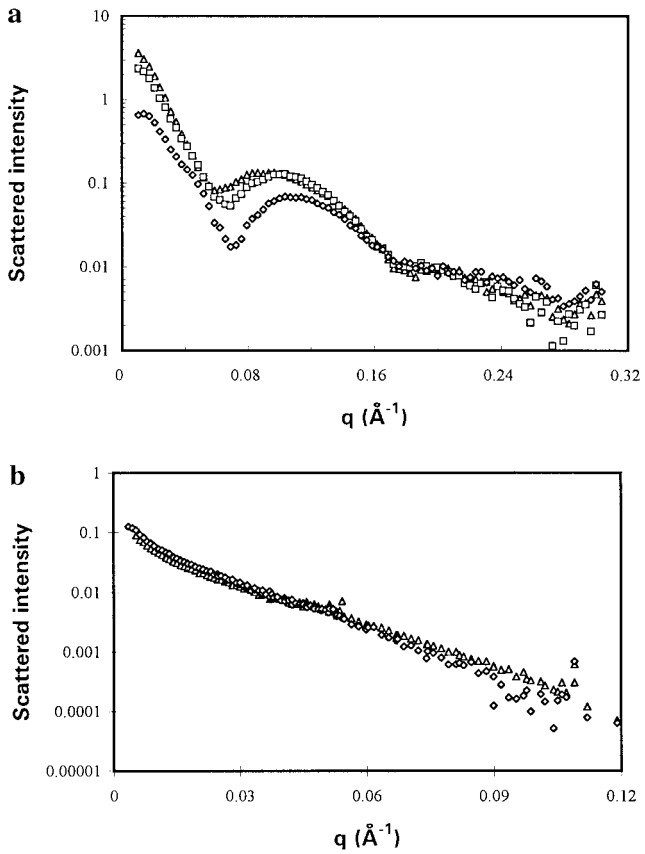

Figure 3. (a) SAXS spectra obtained for the 3 mM GM3 solution at $T = 20$ °C (triangles), $T = 35$ °C (squares), and $T = 50$ °C (diamonds). (b) SANS spectra obtained for the 3 mM GM3 solution at $T = 15$ °C (diamonds) and $T = 45$ °C (triangles).

choline as investigated by osmotic pressure measurements by MacIntosh and Simon.[36] In all these cases, the experimental-results indicate that surfaces coated with the glycolipid experience a steep steric wall extending to larger distances from the hydrophobic−hydrophilic interface than the extended length of the sugar chain headgroup. For example, it has been found that adding GM1 to a lamellar phase of phosphatidylcholine to a molar ratio of 0.3 induces a steep steric wall exceeding 100 atm in osmotic pressure and increasing the repeat lamellar distance by 30 Å. It is then likely to be a property of glycolipids to lean out of flat surfaces, either as single molecules or collectively.

We want to recall here that also as far as the deconvolution of experimental data is concerned, the GM3 bilayer cannot be treated as an usual flat bilayer, which means that not only the results obtained with the procedure including the unconstricted IFT method have to be considered for molecular consistency, but also the usual rules of molecular modeling which are valid for flat bilayers, for which imposing the conservation of volumes ensures also the consistency of lengths, cannot be strictly applied. We have verified that in this case it is rather the comparison between the results coming from the two methods which provides a set of values or trends according to which a picture of the real bilayer can be tried.

(b) Temperature Effect. SAXS and SANS experiments were performed also at different temperatures on the same 3 mM GM3 solution. Figure 3a shows the SAXS data obtained at 20 °C (triangles), 35 °C (squares), and 50 °C (diamonds), while the SANS data at 20 °C (full diamonds) and 45 °C (open triangles) are reported together in Figure 3b. It is easy to appreciate that SAXS spectra show a deeper variation with temperature than SANS ones do.

We recall that for SANS, as already stated, the significant contrast takes place between the hydrophobic inner part of the GM3 bilayer and the solvent, so that the small variation in the SANS spectra of Figure 3b, corresponding to ∼10% variation in σ or, equivalently, in thickness, mainly reflects the behavior of the inner region, being not very much affected by the temperature increase and with a slight trend to be thinner at higher temperatures.

Anyway, as already stated, the variation of the SAXS spectra with temperature is far more significant, indicating, prior to any fitting, that the apolar layer thickness is less sensitive to the temperature variation than the external polar layer, the thinning of which induces the measured shift toward high q's of the oscillation in the high-q region of the SAXS spectra.

Data collected at different temperatures were analyzed by using either the molecular packing constraint and the IFT fitting procedures, with exactly the same steps as described earlier for the data at room temperature.

The molecular model fitting of the SANS and SAXS data obtained at different temperatures was performed by keeping the hydrophobic layer half-thickness, of course the same for SAXS and SANS, to the same value determined at low temperature, $t_1 = 15$ Å. This choice was made following the considerations, expressed so far, about either the low extent of its variation and the fact that the GM3 bilayer cannot be strictly treated with the rules of a flat bilayer, so that it makes little sense to go into more detail. While keeping t_1 fixed, we will then focus our attention on the trends followed by the outer

TABLE 2: Physical Parameters for the GM3 Bilayers at Different Temperatures Obtained from SAXS Data through Molecular Modeling (Normal) and Two-Level IFT (Italics) Methods[a]

	20 °C	35 °C	50 °C
t_1 (Å)	*16*	*16*	*20*
$t_2 - t_1$ (Å)	21 ± 2, *20*	18 ± 2, *16*	15 ± 2, *16*
h	24 ± 3	17 ± 3	9 ± 3

[a] The hydrophobic half-thickness t_1, the hydrophilic layer thickness $t_2 - t_1$, the "hydration" number h, as described in the text. IFT was performed by allowing steps of 4 Å; molecular modeling at different temperatures was performed by keeping the area per headgroup and hydrophobic half-thickness to the values determined at low temperature, $\sigma = 70 \pm 7$ Å^2 and $t_1 = 15 \pm 1.5$ Å.

layer. A noticeable variation in the thickness $t_2 - t_1$ and in hydration number h as a function of temperature was found.

The same data, shown in Figure 3a,b, were then evaluated with the IFT procedure, with the same criteria used for the low-temperature results.

Table 2 summarizes the results obtained at different temperatures in terms of the parameters determined with the two procedures for data evaluation.

The behavior of the GM3 bilayer cross section as a function of temperature can be summarized as a thinning at higher temperatures. By recalling that the large extent of the thickness at low temperature could be explained only by assuming strong deviations from the flat geometry along the bilayer, it follows that an increase in temperature results in a flattening of the GM3 bilayer.

This behavior may, at first, seem surprising, as one normally expects larger fluctuations as temperature increases. For example, undulations, which are of course likely to affect the GM3 bilayer, although not detectable with the kind of experiment performed in this study, usually increase their extent with temperature.

Rather, the observed behavior induces also to exclude that single molecule protrusion is responsible for the features of the cross section profile of the GM3 bilayer, since also molecular protrusion should increase at higher temperatures, rather than decrease.

Then the observed behavior as a function of temperature strongly supports the hypothesis that thickness fluctuations in the form of peristaltic deformations affect the GM3 bilayer, with the following features: (a) they originate from the mismatch between headgroup and chains lateral hindrances, (b) such a mismatch reduces as temperature is raised, resulting in a reduction of the deformation. At higher temperatures, then, the packing geometry of the GM3 monomers becomes more similar to that of the usual flat-bilayer-forming amphiphiles. The phenomenon of the melting of the hydrophobic chains of the GM3 molecule, which takes place over a wide range of temperatures[37] overlapping with the investigated one, is likely to be involved in the modification of the monomer hindrances. The flattening of the bilayer at higher temperatures explains also the dramatic reduction of the estimated water content of the outer layer, put to a noticeably high value at low temperatures in order to account for the external layer volume and contrast, as already mentioned.

Conclusions

This high-resolution SAXS and SANS study drives to draw a picture of the GM3 bilayer structure characterized by strong thickness fluctuations, decreasing their extent as temperature is raised. These results were obtained coherently with a molecular modeling approach as well as an IFT approach for data evaluation. To explain such features, peristaltic deformations, originated by the geometrical properties of the GM3 monomers, are to be imagined to affect the bilayer, besides undulations which are expected and cannot be excluded. Single molecule protrusion cannot explain the temperature behavior of the GM3 bilayer. Interdigitation of the lipid chains together with their full length extension in different places or times across the bilayer is required as a support for the peristaltic deformation. How these microstructural properties are related to adhesion effects, which are at the origin of the importance of glycolipids in immunology, remains to be explored. Osmotic pressure measurements versus temperature and Bragg peak shape in the smectic phase determinations are in progress and are thought to provide some hint in this direction.

Acknowledgment. We would like to thank Otto Glatter for providing the IFT programs as well as for patient initiation to the subtleties of the indirect Fourier transform method and software handling and Sandro Sonnino for providing the needed amount of carefully purified sample and for useful discussions. José Teixeira is thanked for very kind and efficient help for setting up optimized adjustments on PAXE instrument at L.L.B. as well as for comparison of absolute scaling methods. This work was partially supported by Consiglio Nazionale delle Ricerche (CNR), Italy, Special Project Complex Fluids, and by ECC HC&M Project ERBCHRXCT920019 coordinated by D. Langevin.

References and Notes

(1) Tettamanti, G.; Sonnino, S.; Ghidoni, R.; Masserini, M.; Venerando, B. In *Physics of Amphiphiles: Micelles, Vesicles and Microemulsions*; Corti, M., Degiorgio, V., Eds.; North-Holland: Amsterdam, 1985; p 607.

(2) Cantù, L.; Corti, M. In *Nonmedical Applications of Liposomes*; Lasic, D. D., Barenholz, Y., Eds.; CRC Press: Boca Raton, FL, 1996; p 219.

(3) For ganglioside notation, see: Svennerholm, L. *Adv. Exp. Biol. Med.* **1980**, *125*, 11.

(4) Cantù, L.; Corti, M.; Musolino, M.; Salina, P. *Europhys. Lett.* **1990**, *13*, 561.

(5) Sonnino, S.; Cantù, L.; Corti, M.; Acquotti, D.; Venerando, B. *Chem. Phys. Lipids* **1994**, *71*, 21.

(6) Cantù, L.; Corti, M.; Sonnino, S.; Tettamanti, G. *Chem. Phys. Lipids* **1986**, *41*, 315.

(7) Cantù, L.; Corti M.; Acquotti, D.; Sonnino, S. *J. Phys. IV, Colloq. C1* **1993**, *3*, 57.

(8) Cantù, L.; Corti, M.; Del Favero, E.; Raudino, A. *J. Phys. II Fr.* **1994**, *4*, 1585.

(9) Maurer, N.; Cantù, L.; Glatter, O. *Chem. Phys. Lipids* **1995**, *78*, 47.

(10) Cantù, L.; Corti, M.; Del Favero, E.; Maurer, N. *Prog. Colloid Polym. Sci.* **1995**, *98*, 197.

(11) Raudino, A. *J. Phys. Chem.* **1995**, *99*, 152980.

(12) Zemb, Th.; Charpin, P. *J. Phys.* **1985**, *46*, 249.

(13) Cabane, B.; Duplessis, R.; Zemb, Th. *J. Phys.* **1985**, *46*, 2161.

(14) Hayter, J. B.; Penfold, J. *Colloid Polym. Sci.* **1983**, *261*, 1022.

(15) Smith, G. S.; Safinya, C. R.; Roux, D.; Clark, N. A. *Mol. Cryst. Liq. Cryst* **1987**, *144*, 235.

(16) Porte, G.; Appell, J.; Bassereau, P.; Marignan, J. *J. Phys. Fr.* **1989**, *50*, 1335.

(17) Radlinska, E. Z.; Zemb, T. N.; Dalbiez, J. P.; Ninham, B. W. *Langmuir* **1993**, *9*, 2844.

(18) Parsegian, V. A.; Rand, R. P.; Fuller, N.; Rau, D. C. *Methods Enzymol.* **1986**, *127*, 401.

(19) Cantù, L.; Corti, M.; Del Favero, E.; Digirolamo, E.; Sonnino, S.; Tettamanti, G. *Chem. Phys. Lipids* **1996**, *79*, 137.

(20) Cantù, L.; Corti, M.; Del Favero, E.; Digirolamo, E.; Raudino, A. *J. Phys. II Fr.* **1996**, *6*, 1067.

(21) Sonnino, S.; Cantù, L.; Acquotti, D.; Corti, M.; Tettamanti, G. *Chem. Phys. Lipids* **1990**, *52*, 231.

(22) Cantù, L.; Corti, M.; Degiorgio, V. *Europhys. Lett.* **1986**, *2*, 673.

(23) Leflanchec, V.; Gazeau, D.; Tabouri, J.; Zemb, Th. *Appl. Crystallogr.* **1996**, *29*, 1.

(24) Né, F.; Gabriel, A.; Koksis, M.; Zemb, Th. *J. Appl. Crystallogr.*, in press.
(25) Cotton, P. J. In *Neutron, X-ray and Light Scattering*; Lindner, P., Zemb, Th., Eds.; North-Holland: Amsterdam, 1991; p 3.
(26) Porod, G. In *Small-Angle X-ray Scattering*; Glatter, O., Krakty, O., Eds.; Springer: Berlin, 1982.
(27) Glatter, O.; Kratky, O. *Small-Angle X-ray Scattering*; Academic Press: London, 1982.
(28) Glatter, O. *Prog. Colloid Polym. Sci*. **1991**, *84*, 46.
(29) Cantù, L.; Corti, M.; Del Favero, E.; Dubois, M.; Zemb, T. *Biophys. J.* **1998**, *74*, 1600.
(30) J. S.; Schurtenberger, P. *J. Appl. Crystallogr.* **1996**, *29*, 646.
(31) Luckham, P.; Wood, J.; Frogatt, S.; Swart R. *J. Colloid Interface Sci.* **1993**, *156*, 164.
(32) Cantù, L.; Corti, M.; Del Favero, E.; Raudino, A. *J. Phys.: Condens. Matter* **1997**, *9*, 1.
(33) Podgornik, R.; Parsegian, V. A. *Langmuir* **1992**, *8*, 557.
(34) Parker, J. L. *J. Colloid Interface Sci.* **1990**, *137*, 571.
(35) Wood, J.; Luckham, P.; Swart, R. *Colloids Surf. A* **1993**, *77*, 179.
(36) McIntosh, T. J.; Simon, S. A. *Biochemistry* **1994**, *33*, 10479.
(37) Maggio, B.; Ariga, T.; Sturtevant, J. M.; Yu, R. K. *Biochemistry* **1985**, *24*, 1084.